

# Is a Chaotic Multi-fractal Approach for the Temporal Variation of Ozone Concentration Possible ?

Chung-Kung Lee (李中光)

萬能科技大學 綠色環境研發中心及環境工程系 教授

## abstract

One-year series of hourly average ozone observations, which were obtained from urban and national park air monitoring stations at Taipei (Taiwan), were analyzed by means of descriptive statistics and fractal methods to examine the scaling structures of ozone concentrations. It was found that all ozone measurements exhibited the characteristic right-skewed frequency distribution, cycle pattern, and long-term memory. A mono-fractal analysis was performed by transferring the ozone concentration time series (OCTS) into a useful compact form, namely, the box-dimension ( $D_B$ )-threshold ( $T_h$ ) and critical scale ( $C_S$ )-threshold ( $T_h$ ) plots. Scale invariance was found in these time series and the box dimension was shown to be a decreasing function of the threshold ozone level, implying the existence of multifractal characteristics. To test this hypothesis, the OCTS were transferred into the multifractal spectra, namely, the  $\tau(q)$ - $q$  plots. The analysis confirmed the existence of multifractal characteristics in the investigated OCTS. A simple two-scale Cantor set with unequal scales and weights was then used to fit the calculated  $\tau(q)$ - $q$  plots. This model fits remarkably well the entire spectrum of scaling exponents for the examined OCTS. Because the existence of chaos behavior in OCTS has been reported in literatures, the possibility of a chaotic multifractal approach for OCTS characterization was discussed.

*Keywords:* Ozone; Scale invariance; Box-counting; Multifractal scaling analysis; Multifractal cascade model; Chaos

## 1. Introduction

As an indicator component for photochemical smog, ozone is responsible for various adverse effects on human being and foliage. Urban ozone is formed with a complex interaction of temperature, solar radiation,  $\text{NO}_x$ , and VOC's. In Taiwan, the change of ozone and other air pollutants concentration due to human action is measured by Taiwan Air Quality Monitoring Network (TAQMN). The Pollutant Standards Index (PSI) is used to inform the public about the current air quality in respect to its health effects. It is found that in Taipei, two major contributors for the high PSI values (poor air quality) are the  $\text{O}_3$  and PM10. Given the large number of inhabitants and the serious health effects that pollution has on their lives, significant efforts such as the control of nitrogen oxide and volatile organic compounds emissions have been directed to reduce the ozone concentrations. On the other hand, it is also important to develop effective warning strategies from the collected ozone data and weather parameters to reduce impacts to public health during episodes or poor air quality. For this, it is extremely important to understand the dynamics characteristics of ozone from the data recorded at each air quality monitoring station with the aid of different statistical methods.

Generally, the collected ozone data are often recorded as time series and are characterized by many large fluctuations with no obvious autocorrelation (see Figure 1). Moreover, the OCTS usually possess diurnal pattern because the antropogenic influences such as traffic emissions of  $\text{NO}_x$  and VOC's and meteorology have cycle patterns. In the literatures, many researchers have

investigated the dynamics of ozone concentrations from OCTS with different aspects. Among them

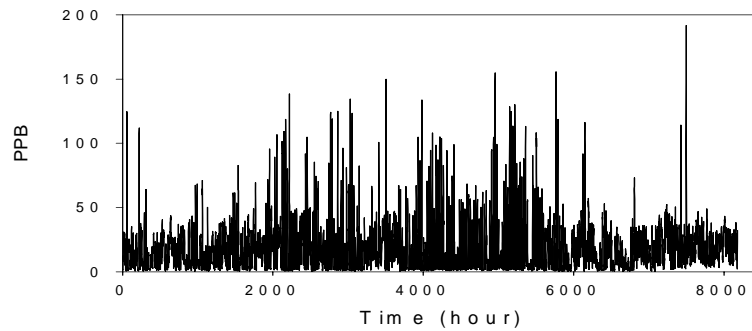


Figure 1

that interest us are the studies using recent advances in nonlinear dynamics and chaos theory to model and predict ozone concentration [1-4]. To obtain more confidence for these approaches, however, it is needed to enhance our fundamental knowledge on the complex structure of ozone history at each station. For this, our previous investigations [5-8] found that the fractal method might be an efficient tool for characterization, analysis, and comparison of the air pollutant concentration temporal characteristics.

In this article, the long-range dependence of OCTS measured at Taipei was first examined with the standard time series analysis. Then, the clustering structure of the time series and its multiscaling characteristics would be analyzed by box-counting technique and multifractal scaling analysis (MSA), respectively. Finally, A simple two-scale Cantor set with unequal scales and weights was used to fit with the obtained multifractal spectra. Based on these results, the possibility of a chaotic multifractal approach for the characterization and prediction of temporal ozone concentration was discussed.

## 2. Materials and methods

### 2.1. Data

At Taipei (Taiwan), the air pollutants concentrations were measured at seven monitoring sites of TAQMN. In this study, only six stations were examined because the ozone concentration was not measured at the traffic station. The selected sites are the urban stations, including the Shin-Lin, Chung-Shan, Wan-Hwa, Ku-Ting, Sung-Shan, and national park station, namely, the Yang-Min station. Our previous investigation [5] found that most examined air pollutant concentration time series in Taiwan exhibited obvious annual periodicity due to the systematic variations in response to seasonal and other factors and the statistical characteristics can be extracted from the data collected over one year. Accordingly, one-year series of hourly average values, from January 1998 to December 1998, was used in this study to examine the scaling characteristics of ozone concentration. It was noteworthy that although a year consists of 8760 hours, only about 8400 readings were collected due to instrument calibration and maintenance. However, the missing observations seemed to be evenly distributed throughout the year.

It is well known that the diurnal and seasonal variations play a significant role in the OCTS. Although they could have a large influence on the results of fractal analysis, however, we still prefer to use the original data to analyze the cluster structure of these time series. The reason is that any data preprocessing may strongly affect the results of fractal analysis and make the interpretation of

the result complex. Moreover, the fractal analysis made below also indicates that the effect of diurnal and seasonal variations on the conclusions is insignificant.

### 2.2. Standard statistical analysis

For the above OCTS, we first evaluated some standard statistical parameters such as coefficient of variation and skewness. The long-range dependency of the time series was examined based on the autocorrelation spectra.

### 2.3. Fractal analysis

The scale invariance in the data set could be detected with the aid of fractal theory. For this approach, some methods have been proposed to estimate the dimension of the data set and the dimension may be interpreted as the degree of irregularity by which the set is distributed. When working with time series, one method is to transform the data into a set of points whose dimension is estimated by box counting [5,6] and other common method is to construct the phase space portrait of the process by using the correlation dimension. Recently, most of the studies have revealed the insufficiency of the above mentioned mono-fractal approaches to characterize the highly irregular time series. Methods suitable for analyzing the multiscaling properties in time series have been suggested, such as moment scaling analysis [5,7-10] and probability distribution multiple scaling. In this study, both the box counting technique and moment scaling analysis are adopted to examine the possible scaling characteristics in the OCTS.

On box-counting method, the space of observation is divided into non-overlapping segments (boxes) of characteristic size  $L$  and the number of boxes  $N(L)$  needed to cover the data set is counted [6]. When applying this method to a time series, the boxes represent time intervals and the space of observation is equal to the total length of the series. To make the ozone concentration into countable items, another step is needed. In this study, we convert the values of the ozone concentration into sets of points (indicating value above threshold,  $T_h$ ) by using different  $T_h$  levels. For this conversion, a zero  $T_h$  means that all hours with a registered ozone concentration in the series are considered a point. If scale invariance exists in the data set, the expression  $N(L) = L^{-D_B}$  will hold, with  $D_B$  as the box dimension. From the time series one can generate a plot of  $\log[N(L)]$  vs.  $\log(L)$  and the exponents  $D_B$  can be obtained from the slope of a linear regression to the values obtained.

Figure 2 shows one typical result of applying the box counting method, using different intensity thresholds, to Sung-Shan monitoring station. Some key features may be observed directly from this figure. The time scale  $L$  denotes a time interval within which ozone concentration exceedances occur and the number of boxes  $N(L)$  is an decreasing function of  $L$ . When  $T_h$  is 0, a linear relationship over the whole scale spectra is observed and the slope is -1. With increasing  $T_h$ , the curve is composed of two distinctly different sections; one with slope equals to -1 and the other with  $-D_B$ . The value of  $L$  at the intersection of these two straight lines corresponds to the critical scale,  $C_S$ . When time scale is greater than or equal to the critical scale,  $C_S$ , the ozone concentration events exceeding the threshold  $T_h$  must occur. On the other hand, the appearance of straight-lined sections with slope  $-D_B$  in the log-log plots suggests the existence of scale invariance within the corresponding time scale range. This result indicates that the examined OCTS can be characterized by a box dimension  $D_B$  or, in other words, display scale invariance within a specific time interval. This is not surprising since the presence of fluctuations at all time scales is in fact the origin of non-trivial scale invariance.

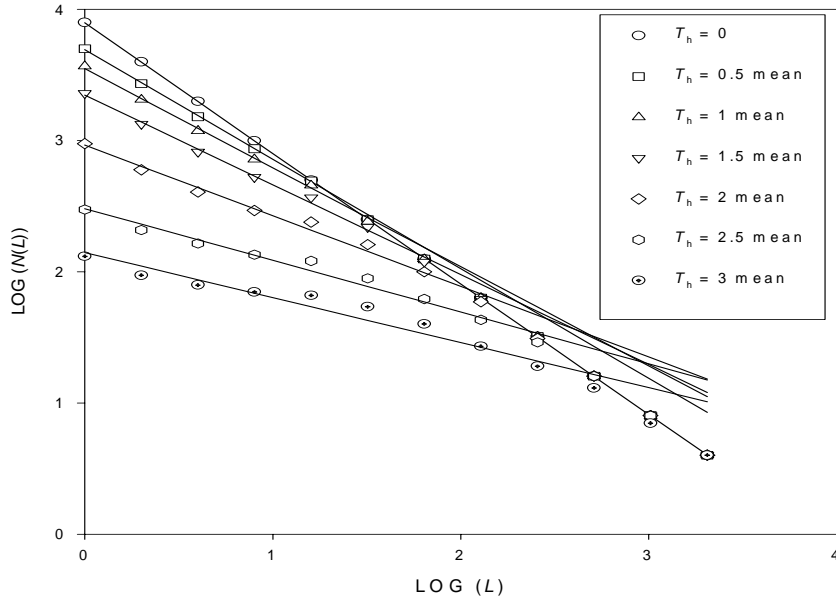


Figure 2

The temporal structure of ozone concentration may depend on the threshold,  $T_h$ ; the higher  $T_h$  the more scattered the pattern and the lower  $T_h$  the more clustered the ozone events. Since the curves are further down and the slopes of the curves are larger (i.e., smaller  $D_B$ ) as  $T_h$  increases, it is concluded that the higher the  $D_B$  the denser the time structure and the lower the  $D_B$  the sparser the time structure. Thus, the  $D_B$  used here reveals the temporal scaling behavior of the ozone concentration point set and is a measure of how the ozone concentration clusters will fill the time axis it occupies. Corresponding to the relationship between  $D_B$  and  $T_h$ , we can also obtain  $C_S$  as an increasing function of  $T_h$ , i.e., a larger time scale is needed to capture an occurrence of higher intensity. Basically, the implication of  $D_B$ - $T_h$  plots is equivalent to that of  $C_S$ - $T_h$  plots, namely, at certain  $T_h$ , a sparser (denser) time structure may be produced with larger (smaller)  $C_S$ , and both contain all information about the ozone point-processes. Thus, with the aid of analysis of both  $D_B$ - $T_h$  and  $C_S$ - $T_h$  plots, some temporal characteristics in OCTS can be identified.

However, it must be remarked that the above approach only gives us information about the global scaling properties of the ozone concentration history. It does not take into account temporal variations of the clustering degree because the local fluctuations of the distribution are not described by a single fractal dimension. Thus, the second method employed is the recently developed multifractal scaling analysis (MSA), i.e., the variability of the distribution at different scales is connected through a dimension function instead of one single dimension [9]. MSA may be used to investigate whether the probability distribution related to different intensity levels is characterized by a scaling behavior. In addition, it must be kept in mind that this approach is able to identify fluctuations existing in distributions but does not indicate where they occur.

Since the detailed information about multifractal procedures can be found elsewhere [7,9-11], we only briefly state the essence of the multifractal formalism used in our analysis. First, the normalized concentration,  $P_{ini}$ , for each hour is determined by  $P_{ini} = \frac{C_{ini}}{\sum C_{ini}}$ , where  $C_{ini}$  is the

ozone concentration at time  $i$ . The series is then divided into nonoverlapping intervals of a certain time resolution,  $T$ . Each interval is characterized by a time resolution  $T$ , and the sum of normalized concentration in the interval, a probability mass function,  $P_j(T)$ . Twelve time resolutions, from  $2^1$  to  $2^{12}$  hour, are considered in this study. A partition function,  $M_q(T)$ , of order  $q$  is calculated from the  $P_j(T)$  values as

$$M_q = \sum_{j=1}^n P_j^q(T) \quad (1)$$

where  $n$  is the total number of the intervals of size  $T$ , and  $q$  is a real number ranging from  $-\infty$  to  $\infty$ . For multifractally distributed measures, the partition function scales with the time resolution as

$$M_q \propto T^{\tau(q)}, \quad (2)$$

where  $\tau(q)$  is the mass exponent of order  $q$ . The mass exponent for each  $q$ -value can be obtained by plotting  $\log M_q(T)$  vs.  $\log T$ . The obtained  $\tau(q)$  may be regarded as a characteristic function of the fractal behavior. If  $\tau(q)$  versus  $q$  is a straight line (convex function) the data set is monofractal (multifractal).

An alternative and equivalent way to study the scaling properties of OCTS is by considering their spectrum of singularities. We assume that in each interval, the mass probability function  $P_j(T)$  increases with the size  $T$  as  $P_j(T) \propto T^\alpha$ , then, the singularity exponent  $\alpha$  is a scaling property peculiar to the interval. The index  $\alpha$  therefore characterizes ‘singularities’ of different strengths and is called a local fractal dimension or a singularity index. It can be determined by Legendre transformation of the  $\tau(q)$  curve as

$$\frac{d}{dq}[\tau(q)] = \alpha(q). \quad (3)$$

Now, corresponding to each  $\alpha$ , one can identify a scaling exponent (or a fractal dimension)  $f(\alpha)$  if one assumes that the number of intervals of size  $T$  with the same  $\alpha$ ,  $N_T(\alpha)$ , is related to the  $T$  as  $N_T(\alpha) \propto T^{-f(\alpha)}$ . Parameter  $f(\alpha)$  can be calculated [10] as

$$\tau(q) = q\alpha(q) - f(\alpha). \quad (4)$$

The shape and the extension of the  $f(\alpha)$ -curve contains significant information about the distribution characteristics of the examined data set. Varying  $q$  is a trick for exploring the different regions of  $\alpha$ . For large and positive  $q$ , we are looking for small values of  $\alpha$ ; i.e., parts of the measure in which the  $P_{ini}$  values is high. For large and negative  $q$ , we study parts of the object for which the measure is very small and corresponds to the larger value of  $\alpha$ . On the other hand, low values of  $f(\alpha)$  characterize a rare occurrence of isolated peaks in a data sample, high values of  $f(\alpha)$  a more frequent and dense appearance of data values. In general, the spectrum has a concave downward curvature, with a range of  $\alpha$ -values increasing correspondingly to the increase in the heterogeneity of the distribution. For  $q = 0$ , we can deduce  $\tau(0) = -D_0$ , where  $D_0$  is the fractal dimension of the support of our measure and is equal to 1.0 because we are dealing with a one-dimensional data support (1-D time series). This turns out to be the maximum possible value of  $f$ . For a homogeneous distribution, the  $\tau(q)$ - $q$  curve becomes linear and then  $f = \alpha = D_0$ , i.e.,  $D_0$  is also the fractal dimension of all the subsets.

#### 2.4. Multifractal cascade model

A simple generalized Cantor set with two rescaling parameters ( $l_1$  and  $l_2$ ) and measure parameters ( $p_1$  and  $p_2$ ) was adopted to model the multifractal spectra of OCTS [7]. In this study, we assume  $l_1 + l_2 = 1$  (because we are dealing with a one-dimensional data support) and  $p_1 + p_2 = 1$ , respectively. The two-scale Cantor set is constructed on an interval  $E$  of unit length, where  $E_0 = E$ ,  $E_n$  contains  $2^n$  subintervals obtained by dividing each subinterval of  $E_{n-1}$  into two different length intervals. The positive measure  $\mu$  on  $C$  is defined as follows. We start with the original region which has measure 1 and size 1 (i.e.,  $E_0 = 1$  and  $\mu_0 = 1$ ). At the second stage, the unit mass and size are split into  $p_1$  and  $p_2$  as well as  $l_1$  and  $l_2$ , respectively. This defines  $\mu_1$ , which has  $p_1$  on one interval ( $l_1$ ) and  $p_2$  on the other interval ( $l_2$ ). Continue in this way, the mass on each interval of  $E_n$  will be divided randomly into the proportions  $p_1$  and  $p_2$  between its two subinterval in  $E_{n+1}$ . Accordingly, a sequence  $\{\mu_n\}$  can be defined and it will converge weakly to a limiting mass distribution  $\mu$  on  $C$ .

Because for each  $0 \leq m \leq n$ , a number  $\binom{n}{m}$  of the  $2^n$  intervals of  $E_n$  have mass  $p_1^m(p_2)^{n-m}$ , it is apparent that the  $P_j(T)$  is generated by a multiplicative cascade with a binomial generator characterized by a probability  $p_1$ .

In this study, the  $P_j(T)$  is assumed to be generated by such an recursive process and its scaling is described by equation (2). To test the validity of the multiplicative cascade model on simulating the ozone concentration data set, both the  $\tau(q)$  and  $f(\alpha)$  functions are needed to determine. For this generalized two-scale Cantor set, the analytic expressions for both the  $\tau$ - $q$  and  $f$ - $\alpha$  curves have been obtained by Halsey et al. [11]:

$$\tau = \frac{\ln\left(\frac{n}{m} - 1\right) + q \ln\left(\frac{p_1}{p_2}\right)}{\ln\left(\frac{l_1}{l_2}\right)}, \quad (5)$$

$$\alpha = \frac{\ln p_1 + \left(\frac{n}{m} - 1\right) \ln p_2}{\ln l_1 + \left(\frac{n}{m} - 1\right) \ln l_2}, \quad (6)$$

$$f = \frac{\left(\frac{n}{m} - 1\right) \ln\left(\frac{n}{m} - 1\right) - \left(\frac{n}{m}\right) \ln\left(\frac{n}{m}\right)}{\ln l_1 + \left(\frac{n}{m} - 1\right) \ln l_2} \quad (7)$$

For any given  $q$ , the  $\tau$ ,  $\alpha$ , and  $f$  could be determined by eliminating  $\frac{n}{m}$  with the aid of the following equation

$$\ln\left(\frac{n}{m}\right) \ln\left(\frac{l_1}{l_2}\right) - \ln\left(\frac{n}{m} - 1\right) \ln l_1 = q(\ln p_1 \ln l_2 - \ln p_2 \ln l_1). \quad (8)$$

Because the equations (5) to (7) are highly nonlinear, the effects of  $l_1$  and  $p_1$  on both  $f$ - $\alpha$  and  $\tau$ - $q$  curves can only be obtained by solving those equations numerically. Our previous investigation [7] found that larger  $p_1$  and smaller  $l_1$  might produce more obvious curvature at  $\tau$ - $q$  curve. Since higher non-linearity of the  $\tau(q)$  curves is translated into a wider  $f(\alpha)$  dispersion, then more pronounced multifractal characteristics,  $p_1$  and  $l_1$  may be used to compare the distribution's heterogeneity in the examined OCTS.

### 3. Results

#### 3.1. Standard statistical characteristics

The standard statistical parameters estimated from the OCTS are shown in Table 1. For all examined stations, both the mean values and coefficients of variation are nearly equal (except Yang-Min), indicating that the spatial differences in ozone concentration at Taipei are rather small. On the other hand, the mean value of Yang-Min (national park station) is larger than that of other urban stations. One way to explain this result is that although urban stations may possess higher ozone concentration at some times due to the higher precursor concentration ( $\text{NO}_x$ , and VOC's), it may also have higher  $\text{O}_3$  dissipating rate owing to the higher concentrations of other air pollutants which may react with ozone. Accordingly, the mean values of ozone concentration at urban stations are lower than that of Yang-Min and the variation of ozone concentration at urban stations may be larger than that of Yang-Min, as indicated by the coefficients of variation in Table 1. Finally, because the coefficients of skewness of all examined stations are positive, the ozone distributions are all right-skewed. Moreover, the right-skewness degree of frequency distribution of the examined

stations are also alike (except for Yang-Min and Shin-Lin).

Table 1. Basic statistical properties and multifractal cascade model parameters of the examined OCTS.

Monitoring Station	Mean (ppb)	Coeff. of variation	Coeff. of skewness	$p_1$	$l_1$	Range of $\alpha$
Shin-Lin	18.4	0.84	0.91	0.510±0.001	0.385±0.001	0.751
Chung-Shan	16.2	1.05	2.06	0.504±0.001	0.403±0.001	0.589
Wan-Hwa	18.8	1.02	2.19	0.500±0.001	0.425±0.001	0.404
Ku-Ting	16.7	1.01	2.26	0.501±0.001	0.413±0.001	0.499
Sung-Shan	17.2	1.09	2.31	0.500±0.001	0.420±0.001	0.435
Yang-Min	40.3	0.38	0.29	0.500±0.001	0.436±0.001	0.329

The autocorrelation spectra given in Figure 3 indicate a clear diurnal pattern (except Yang-Min) due to the fact that both traffic emissions of NO<sub>x</sub> and VOC's and meteorology have cycle patterns. For Yang-Min, the disappearance of cycle pattern reveals that the precursor pollutants (NO<sub>x</sub>, and VOC's) for the ozone formation are insufficient and the ozone in Yang-Min is mainly contributed from the diffusion of ozone generated at surrounding areas (especially Taipei city). Moreover, the autocorrelation functions of all examined OCTS decrease slowly in a manner that is certainly different from an exponential decay. This slow decay in the autocorrelation function indicates a

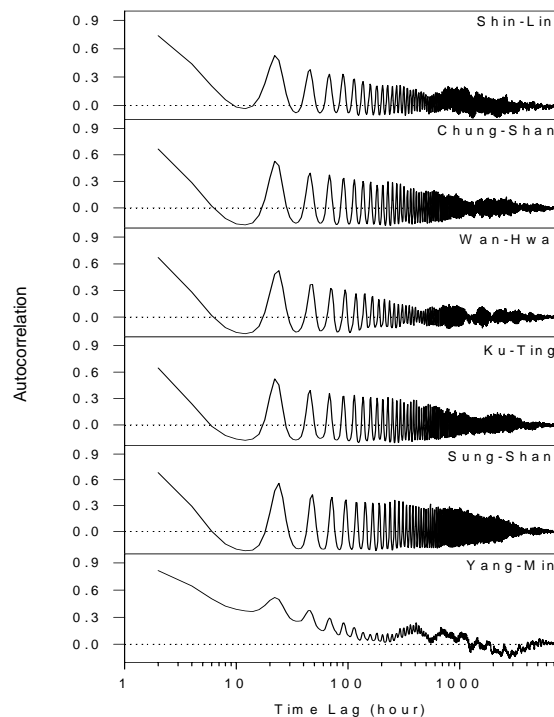


Figure 3

temporal persistence that may be related to self-similar properties in the time series.

### 3.2. Box Dimension

Figure 4 shows both  $D_B-T_h$  and  $C_S-T_h$  plot for all examined monitoring stations. As demonstrated in Figure 4(a), the plots could be roughly divided into two groups, Yang-Min and other urban stations. Under a certain  $T_h$  value, the  $D_B$  values of Yang-Min are larger than that of urban monitoring stations. Above a certain  $T_h$  value, we get the opposite result to the former case. At low  $T_h$  (0-0.5 mean), the low decrease of  $D_B-T_h$  plot of Yang-Min indicates that at low

concentration, its pattern is more discrete and the persistence of occurrence is less continuous than

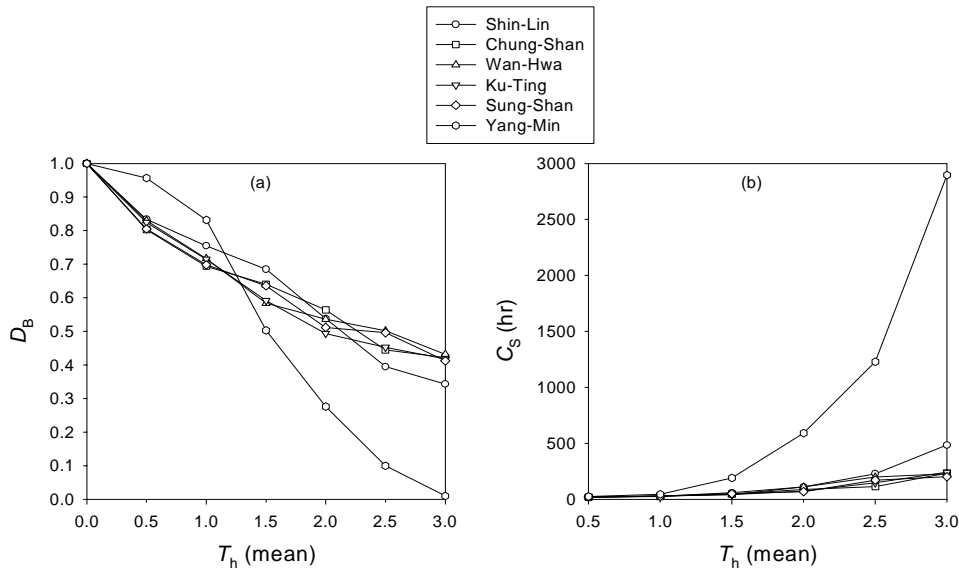


Figure 4

other urban monitoring stations. At high  $T_h$  ( $>3$  mean), Yang-Min still possess a less dense and continuous pattern due to possessing smaller  $D_B$  and the fast decrease of  $D_B$ - $T_h$  plots at intermediate  $T_h$  (1-3 mean). Another way to say about this result is that during a longer (or shorter) period, the high (or low) concentration events occur more difficult for Yang-Min than for other urban monitoring stations (see Figure 4(b)). Therefore, it may be concluded that the data of Yang-Min are more concentrated on middle concentration regions but not on low and high range.

It is apparent that both  $D_B$ - $T_h$  and  $C_S$ - $T_h$  plots are closely related to the concentration variation of ozone. Thus, it is interesting to discuss the correlation between  $D_B$ - $T_h$  ( $C_S$ - $T_h$ ) plot and the coefficient of variation. As mentioned earlier, when the ozone data has larger  $D_B$  at low  $T_h$  and smaller  $D_B$  at high  $T_h$ , its distribution will concentrate on middle concentration regions but not low and high range. In this case, it will possess smaller temporal variation, namely, smaller coefficient of variation. Therefore, Yang-Min station may have smaller concentration variation when comparing with urban monitoring stations. This result is consistent with the coefficients of variation shown in Table 1. Although both  $D_B$ - $T_h$  and  $C_S$ - $T_h$  plots are closely related to the coefficient of variation, it is noteworthy that the former provides a much deeper insight into data structure than the latter because it can present a more microscopic picture about the distribution of data set. On the other hand, if we take closer look at the  $D_B$ - $T_h$  plots and the corresponding coefficients of skewness in Table 1, some interesting correlations can also be found. Generally, the coefficient of skewness gives a measure of the relative skewness of a distribution. For distributions that have tails extending to the right, the coefficient of skewness is positive and the distribution is called right-skewed. For a right-skewed distribution with a single mode, the location of the mean is at the right side of the mode. Moreover, when the location of the mode moves more to the left, the larger is the coefficient of skewness. Accordingly, for a right-skewed distribution the  $D_B$ - $T_h$  plot will show a sharp decrease when  $T_h < 1$  mean and the larger the decreasing rate of  $D_B$ , the larger is the coefficient of skewness. As demonstrated in Figure 4(a), when  $T_h < 1$  mean, the  $D_B$ - $T_h$  plots of all examined monitoring stations show pronounced decrease, indicating that the distributions of all examined OCTS are right-skewed. Moreover, the coefficient of skewness of Yang-Min station is the smallest among the examined monitoring stations (see Table 1), which is consistent with the slowest decreasing rate of  $D_B$  at low threshold ( $T_h < 1$  mean) when comparing with other monitoring stations.

The existence of close relationship between the  $D_B$ - $T_h$  plots and the coefficients of variation



and skewness may provide some basis for the validity of box counting technique used in this study. This also indicates that the box counting is a useful approach to identify the temporal variation of ozone data. On the other hand, because scale invariance is closely related to the long-range dependence in the data set, it is not adequate to treat the ozone distribution as an independent stochastic process. This also indicates that the Poisson distribution, which assuming the occurrence of the event is completely random in a certain time interval, is not appropriate.

Finally, the results of the mono-fractal analysis presented above show that a single dimension is insufficient to describe the scaling properties of the OCTS. It is found that the values of  $D_B$  (or  $C_S$ ) decrease (or increase) as the  $T_h$  magnitude increases, implying that different threshold intensities reveal different properties of the OCTS. Thus, a multifractal approach may be more suitable for describing the OCTS [5,7].

### 3.3. Multifractal scaling analysis

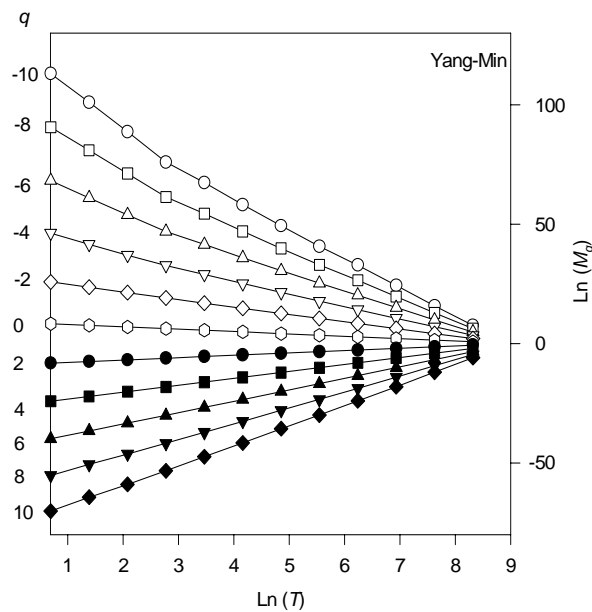


Figure 5

Shown in Figure 5 are plots of the  $q$ th-order moment  $M_q$  vs. the time scale  $T$  in a log-log scale. All of these plots are mostly close to being straight for  $-10 \leq q \leq 10$ , signifying that the studied OCTS can be regarded as multifractal measures. The observation of multifractal scaling in OCTS is encouraging since multifractal formalism has been successfully applied to systems as complex as turbulence, and it may also have a great potential in modeling the complex structure of ozone. Before this can be done, however, a physical interpretation must be made concerning which ozone generating processes that can lead to such multifractal characteristics. When applying a multiscaling approach to temporal clustering of earthquakes, multifractal characteristics are interpreted in terms of diffusive processes of stress in the Earth's crust. Moreover, multifractal characteristics in rainfall data have been explained with an assumption that a large-scale flux is successively broken into smaller and smaller cascades, each receiving an amount of the total flux specified by a multiplicative parameter. On the other hand, the multifractal characteristics in stock market are interpreted with the random multiplicative process of market information [10]. It is noteworthy that the stochastic processes proposed for above systems to generate multifractal characteristics are closely related to the heart of turbulence, namely, the multiplicative cascade process. The only difference is the characteristic physical quantity accompanying in the stochastic processes. For

earthquakes, rainfall, stock market, and turbulence, the corresponding characteristic quantity is stress, water, market information, and energy, respectively. Accordingly, the multifractal characteristics in OCTS may be interpreted with the aid of random multiplicative process of ozone concentration [5,7].

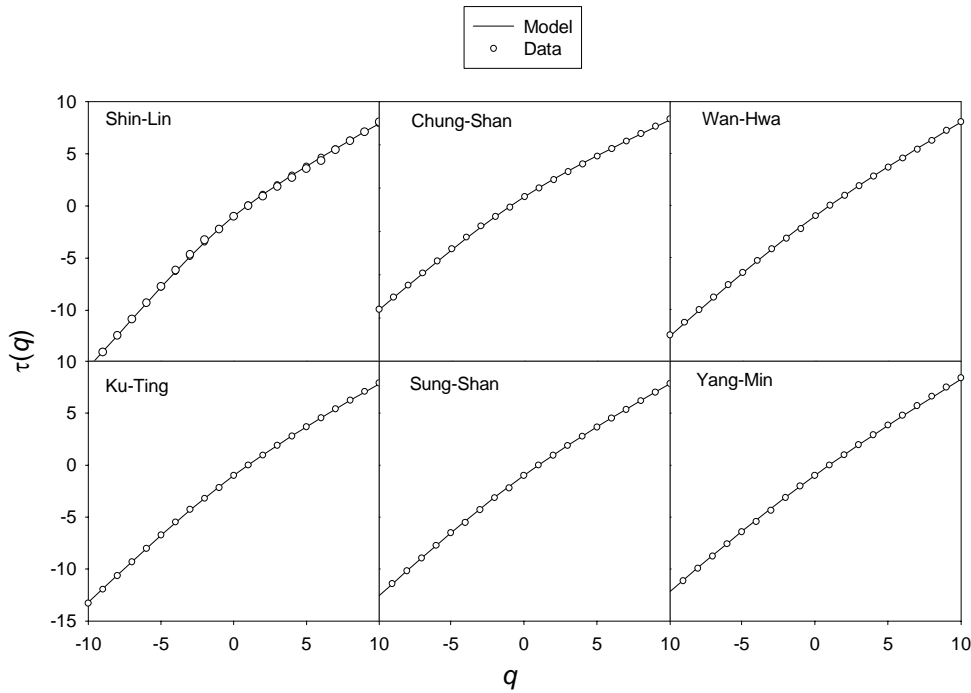


Figure 6

Since multifractal characteristics indeed exist in all examined OCTS and can be viewed as a result of random multiplicative process, we next fit multifractal cascade model to these experimental  $\tau(q)$  curves. The values of  $p_1$  and  $l_1$  can be estimated by comparing the experimental  $\tau(q)$  curves with the curves computed from model for a range of values of  $p_1$  and  $l_1$ . In Figure 6, we show a comparison between the measured  $\tau(q)$  curve and equation (5) for all examined monitoring stations. The agreement is remarkable and the estimated  $p_1$  and  $l_1$  parameters are shown in Table 1. It is worth mentioning that if we use equal scales, i.e.,  $l_1 = l_2 = 0.5$ , no choice of  $p_1$  would have been satisfactory. Since both  $p_1$  and  $l_1$  are determined, the corresponding  $f(\alpha)$  curves can be obtained with the aid of equations (6) and (7). As demonstrated in Figure 7 and Table 1, the  $\alpha$  range, then the multifractal characteristics (or the distribution's heterogeneity), increases with the order: Yang-Min < Wan-Hwa < < Sung-Shan < Ku-Ting < Chung-Shan < Shin-Lin. As mentioned earlier, larger  $p_1$  and smaller  $l_1$  may correspond to stronger multifractal characteristics. Accordingly, as shown in Table 1 and Figure 7, the multifractal property (or the distribution's heterogeneity) of Yang-Min may be less obvious than that of urban stations. Moreover, it should be noteworthy that on multifractal analysis,  $\alpha$  dispersion strength represents the range between the high and low ozone value, as well as the number of high and low concentration data are related to the left and right parts of the  $f(\alpha)$  spectrum, respectively. Because the variations of data set is determined by both the data values and their corresponding number, the range of  $\alpha$  itself is insufficient to determine the relative variability when comparing different data set. This is why the  $\alpha$  range of Shin-Lin is the largest but

its coefficient of variation is not the largest among the examined stations. This result also indicates that multifractal approach provides a much deeper insight into data structure than the coefficient of variation because it can provide a more microscopic picture about the distribution of data set.

#### 4. Discussion and Conclusions

Some statistical methods have been used to investigate the clustering properties of OCTS in Taipei. The autocorrelation of all OCTS do not decay to zero exponentially but in a slower manner, indicating a temporal persistence in the examined OCTS. The scaling characteristics are first identified with the aid of box-counting technique. Multifractal analysis further indicates that the OCTS could be viewed as multifractal measures that may be the result of a random multiplicative process. A simple two-scale Cantor set with unequal scales and weights is then presented for the OCTS. This model fits remarkably well the entire spectrum of scaling exponents for the examined OCTS. The validity of fractal approach is supported with the existence of close relationship between the practical implications of  $D_B-T_h$  plots ( $l_1$  and  $p_1$ ) and the traditional statistical parameters.

Although the fractal characteristics in OCTS are hardly reported in the literature and the studies conducted over the past several decades on air pollution have indicated no evidence of a deterministic behavior, it has been increasingly realized that the seemingly irregular-looking dynamic behavior of ozone could be the result of a simple deterministic system influenced by only a few nonlinear interdependent variables with sensitive dependence on initial conditions, i.e., chaos theory. The papers by Lee et al. [3], and Raga and Le Moyne [4] have shown possible presence of chaotic dynamics in hourly ozone concentration. Chen et al. [1] and Kocak et al. [2] have performed a nonparametric short-term prediction successfully by using the chaos theory. However, none of the past studies that investigated the existence of chaos in an OCTS attempted to investigate the existence of fractal behavior.

The validity of fractal approaches shown in the present investigation and chaos characteristics in OCTS identified with other researchers may provide positive evidence regarding the coexistence of multifractal and chaotic behaviors in the OCTS. This result is similar to the recent observation by Sivakumar [12] for rainfall process. He pointed out that multifractal approaches might provide positive evidence of a multifractal nature not only in stochastic processes but also in chaotic processes. A possible implication of this might be that OCTS characterization could be viewed from a new perspective: the chaotic multifractal perspective. It should be noted, however, that the methods and approaches employed in the present study possess some limitations. For instance, although the two-scale Cantor set can be regarded as a convenient model for ozone distribution in time, especially, if one is interested in modeling correctly the scaling properties of OCTS, it is difficult to conclude that the ozone distribution is governed exactly by a single two-scale Cantor set with  $p_1$  and  $l_1$  as parameters. Moreover, the studies to investigate the presence of both fractal and chaotic behaviors in the same OCTS are still needed. Therefore, the results obtained here should be substantiated further using chaos and other fractal identification methods to offer sound proof regarding the coexistence of fractal and chaotic nature in OCTS. Investigation in this direction is now in progress.

#### Acknowledgements

The work is supported by the grant NSC91-2211-E238-001 of National Science Council (Taiwan, ROC) and the data are supplied by the Environmental Protection Administration of ROC.

#### References

1. Chen, J.-L., S. Islam, P. Biswas, "Nonlinear dynamics of hourly ozone concentrations: nonparametric short term prediction," *Atmospheric Environment*, 32, 1839-1848 (1998).
2. Kocak, K., L. Saylan, O. Sen, "Nonlinear time series prediction of  $O_3$  concentration in Istanbul,"

Atmospheric Environment 34, 1267-1271(2000).

3. Lee, I.F., P. Biswas, S. Islam, "Estimation of the dominant degrees of freedom for air pollutant concentration data: applications to ozone measurements," Atmospheric Environment 28, 1707-1714(1994).
4. Raga, G.B., L. Le Moyne, "On the nature of air pollution dynamics in Mexico City-I. Nonlinear analysis," Atmospheric Environment, 30, 3987-3993(1996).
5. Lee, C.K., "Multifractal characteristics in air pollutant concentration time series," Water, Air & Soil Pollution, 135 (1-4), 389-409 (2002).
6. Lee, C.K., D.S., Ho, C.C., Yu, C.C., Wang, "Fractal analysis of temporal variation of air pollutant concentration by box counting," Environmental Modelling & Software, 18, 243-251(2003).
7. Lee, C.K., D.S., Ho, C.C., Yu, C.C., Wang, T.H., Hsiao, "Simple multifractal cascade model for the air pollutant concentration time series," Environmetrics, 14, 255-269 (2003).
8. Ho, D.S., L.C. Juang, Y.Y. Liao, C.C. Wang, C.K. Lee, T.C. Hsu, S.Y. Yang, "The temporal variations of PM10 concentration in Taipei: fractal approach," Aerosol and Air Quality Research, 4(1), 37-54(2004).
9. Lee, C.K., S.L., Lee, "Heterogeneity of surfaces and materials, as reflected in multifractal analysis," Heterogenous Chemistry Reviews, 3, 269-302(1996).
10. Ho, D.S., C.K. Lee, C.C. Wang, M. Chuang, "Scaling characteristics in the Taiwan stock market," Physica A 332, 448-460(2004).
11. Halsey, T.C., M.H. Jensen, L.P. Kadanoff, I. Procaccia, B.I. Shraiman, "Fractal measures and their singularities: the characterization of strange sets," Physical Review A 33, 1141-1151(1986).
12. Sivakumar, B., "Is a chaotic multi-fractal approach for rainfall possible?" Hydrological Process 15, 943-955(2001).

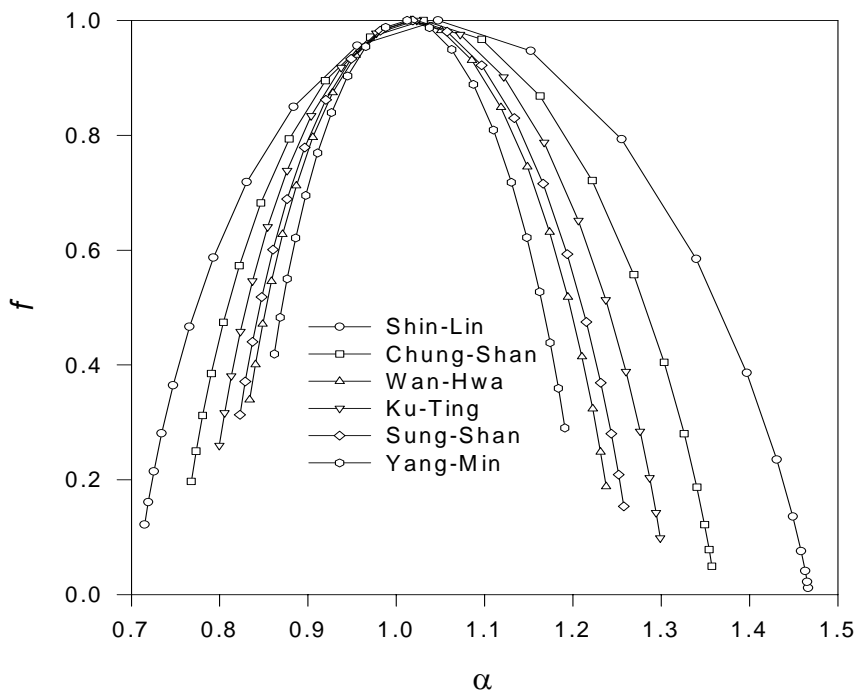


Figure 7